The Generation Mechanism of the Western Disturbances over the Himalayas

Masayuki Hara*, Fujio Kimura,* and Tetsuzo Yasunari,*

*Frontier Research Center for Global Change,

Japan Agency for Marine-Earth Science and Technology,

e-mail: hara.masayuki@jamstec.go.jp

†Institute of Geoscience, University of Tsukuba

‡Hydrospheric Atmospheric Research Center, Nagoya University

Abstract

A meso-α-scale quasi-stationary cyclone sometimes appears along the southern slope of the Himalayas. The cyclone can be simulated reasonably well by a regional meteorological model and can be explained by the theory of the topographic Rossby wave. The characteristics of the cyclone were also verified using an f-plane shallow-water equations model (SWEM). The model studies suggest that the cyclone is generated when a synoptic trough passes over the Tibetan plateau. The southern part of the trough is cut off at the western side of the plateau and forms a cyclone. Although the generated cyclone is almost stationary and moves eastward very slowly, the remaining northern part of the trough moves eastward faster than the subtropical westerlies. These properties can also be seen in the results of the SWEM simulations. The vertical structure of the cyclone is barotropic and extends up to the tropopause. The phase velocity and vertical/horizontal structure of the cyclone agree well with the theoretical solution of the topographic Rossby wave in a stratified quasi-geostrophic fluid.

1 Introduction

A meso-α-scale quasi-stationary cyclone sometimes appears along the southern slope of the Himalayas and occasionally brings heavy snowfall. In the winter of 1990/1991, the most tragic accident in the history of mountaineering occurred in Meilixueshan in southeastern Tibet. Because of the abnormally heavy snowfall for a full two-to-three-day period between January 1 and 3, 1991, a huge avalanche that was triggered near the summit of the mountain hit an expedition camp and killed seventeen climbers. The new snow that had accumulated during the two-to-three-day snow period was estimated to be more than two meters in depth; however, the meteorological disturbance directly responsible for the heavy snowfall had not been clearly detected in the synoptic weather chart (Sakai, 1991). This study determined that the cyclone had been triggered by the trough to the west of the plateau and had propagated very slowly as a topographic Rossby wave (TRW) along the southern periphery of the Tibetan plateau and the Himalayan range.

In the ocean, TRWs are sometimes observed and have been studied well (Rhines, 1969; Pedlosky, 1987). Although TRWs can theoretically exist in the atmosphere as well, little observational evidence has been presented so far. TRWs can be explained by the conservation law of potential vorticity as an oscillation of the relative vorticity caused by the bottom slope. On the other hand, Rossby β-waves are explained as the oscillation of the relative vorticity contributed by the β effect.

In the northeast region of the Tibetan plateau, a cold surge is observed after a synoptic trough passes over the plateau (Nakamura and Doutani, 1985). Naka-mura and Doutani (1985) studied the cold surge around the Tibetan plateau with a numerical model and indicated that the dynamics of the Kelvin wave and TRW are some of the major factors responsible for the generation of the cold surge. Hsu (1987) studied storm tracks around the major mountains in the world and stated that the statistical features of the storms propagating along the mountain ranges are similar to those of TRWs. However, the disturbances observed in the
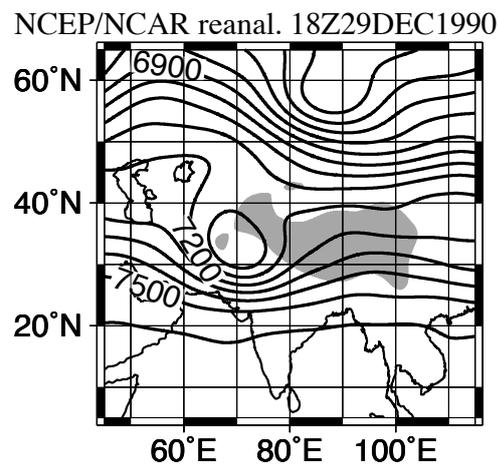
NCEP/NCAR reanal. 18Z29DEC1990

Figure 1: Geopotential height at 400 hPa at 18 UTC December 29, 1990; NCEP/NCAR reanalysis dataset. The shaded area indicates the area in which the topographical height is greater than 2500 m.

northeast of the Tibetan plateau can be explained as a mixed mode of coastal Kelvin waves and TRWs. Coastally trapped waves (CTWs) in the atmosphere are often observed and studied. For major mountains

around the world, such as the Rockies, the Alps, and Southern Africa, there are many studies about CTWs (Tory et al., 2001; Gross, 1994; Gill, 1977).

Meso-α-scale quasi-stationary cyclones, called Western Disturbances, are sometimes observed along the southern slope of the Himalayas. By means of a statistical analysis using the station data and the NCEP/NCAR reanalysis data, Lang and Barros (2004) demonstrated that cyclones exist in the southwestern area of the Himalayas in snow days in the central Himalayas, but they did not explain why cyclones occur and stay in the area. In this paper, we will explain why cyclones occur and stay in the southwestern area of the Himalayas using the theory of TRWs.

Figure 1 shows the contours of the geopotential height at the level of 400 hPa at 18UTC December 29, 1990, three days before the abovementioned accident, given by NCEP/NCAR reanalysis data (Kalnay et al., 1996). The early stage of the cyclone, which later brought the disaster mentioned above, seems to be one of the typical cases of the southwest cyclone. A cyclone exists in the southwestern side of the Tibetan plateau. The horizontal scale of the cyclone extends to 1400 km, and the cyclone has a barotropic vertical structure in the troposphere. Although the strong subtropical westerly blows in this area, this cyclone propagated eastward very slowly along the Himalayas and survived for a week.

2   Realistic Numerical Simulation

The numerical model in the present study is a modified RAMS (TERC-RAMS, Pielke et al., 1992; Yoshikane et al., 2001; Sato and Kimura, 2003). NCEP/NCAR reanalysis data was used as initial and lateral boundary conditions. The lateral boundary conditions are interpolated 6-hourly from NCEP/NCAR reanalysis data. The sea surface temperature is interpolated from the monthly mean data of Reynolds SST (Reynolds, 1994). The horizontal grid interval is 100 km (100×100 grid points), while the vertical grid interval is 120 m in the lowest layer stretching gradually to increase up to 1000 m in the upper layer (30 layers together). The numerical experiment started at 0 UTC December 27, 1990 and ran until 0 UTC January 1, 1991. Full physics are assumed in all of the three experiments.

Figure 2 shows the geopotential height at the level of 400 hPa at every 30 hours from 6 UTC December 28 to 6 UTC December 29, 1990 simulated by the CONTROL run. In comparison with the reanalysis data, the time evolution and spatial structure of the quasi-stationary cyclone seem to be reasonably simulated by the CONTROL run. In the middle level of the troposphere, the synoptic trough is located in the west of the Tibetan plateau (Fig. 2A, 6 UTC December 28, 1990). When the synoptic trough hits the Tibetan plateau, the southern part of the trough is cut off, and a cyclone is generated in the southwest area of the plateau (Fig. 2B, 18 UTC December 29, 1990). At the same

time, this cyclone causes snowfall along the Himalayas (no figure). The generated cyclone propagates eastward very slowly accompanied by precipitation along the Himalayas and survives for a week (Fig. 2C, 6 UTC December 31, 1990). Although the averaged westerly in this area is estimated to be about 25 m/s in the middle level in the troposphere, the eastward migration speed of the cyclone is only about 4 m/s.
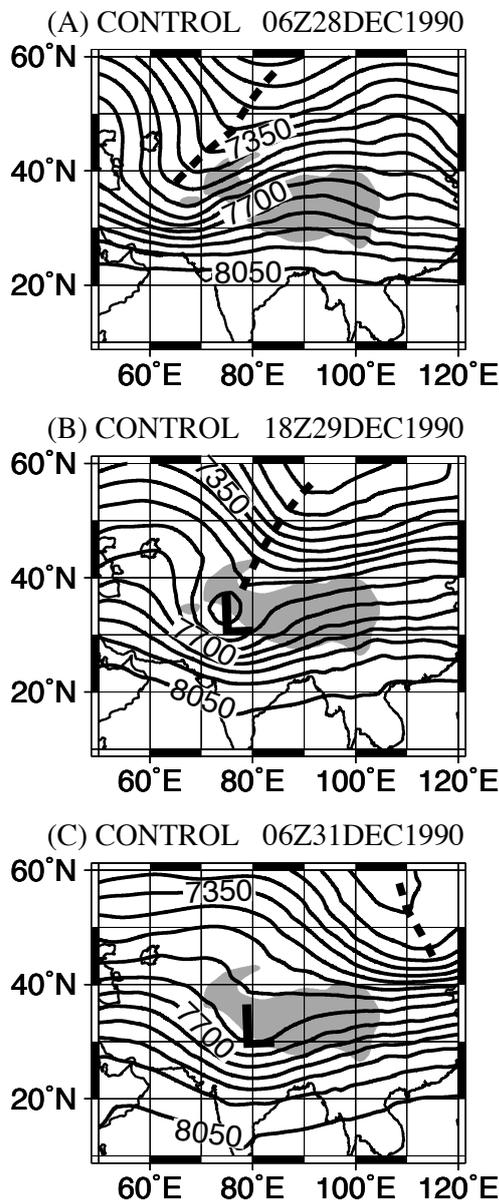

Figure 2: Geopotential height at 400 hPa simulated by the TERC-RAMS/CONTROL run at (A) 6 UTC December 28, (B) 18 UTC December 29, and (C) 6 UTC December 31, 1990. The thick line indicates the location of the synoptic trough, 'L' shows the center of the cyclone, and the shaded area indicates the area in which the orographic height is greater than 2500 m.

Figure 3 shows a longitude-vertical cross section of the meridional wind and relative vorticity at 18 UTC December 29, 1990. The vertical distribution of the relative vorticity and the meridional wind at the center of

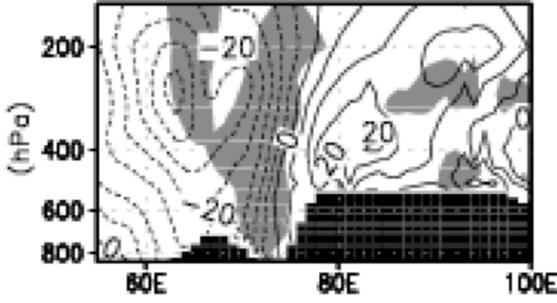the cyclone indicates that the cyclone has a barotropic structure.

Figure 3: Vertical-longitude cross section at 34 °N of the meridional wind and relative vorticity of the CONTROL run at 18 UTC December 29, 1990. The contours indicate meridional wind, and the gray shaded area indicates the area in which the relative vorticity is greater than 0.5×10^{-4} s^{-1}.

3 Discussion

The structure of TRWs in the ocean has been revealed in studies by Rhines (1969) and Pedlosky (1987). In the stratified quasi-geostrophic fluid, the phase speed of TRWs over the bottom is given as

$$c = u_0 - \frac{s \cdot f_0}{h_0} \cdot \frac{1}{K^2}, \qquad (1)$$

where c is the phase speed of TRWs, f_0, the Coriolis parameter, s, the gradient of the bottom slope, h_0, the averaged depth of fluid, K, the horizontal wave number, and u_0, the mean meridional wind velocity. The vertical scale of TRWs depends on its horizontal scale and phase speed. The vertical e-folding scale of TRWs (d) in a nearly neutral state is given as follows,

$$d = \frac{1}{K} \cdot \frac{f_0}{N}, \qquad (2)$$

where N is the Brunt-Väisälä frequency.

The phase speed of TRWs in a shallow-water equations system can also be estimated by Equation (1).

From theoretical Equation (1), the phase speed of the TRW is estimated to be about 20 m/s westward, and the phase speed of the TRW against the earth is estimated to be 5 m/s eastward. This value almost agrees with the 4 m/s estimated by the numerical model. By the linear theory, the phase speed of the Rossby β-wave in this region is 0.26 m/s westward against the atmosphere. The Rossby β-wave cannot explain the cyclone along the Himalayas because it is too slow.

The vertical scale of the TRW can be theoretically estimated with the Coriolis parameter and the atmospheric static stability. After the theory assuming a stratified fluid and a quasi-geostrophic approximation, the vertical scale of the TRW is related with the horizontal scale of the TRW, as given by Equation (2).

Since it is estimated to be about 4.5×10^4 m, the vertical structure of the TRW should almost be barotropic in the troposphere. In estimating the phase speed of the TRW, we use the height of the tropopause as the depth of fluid because the observed disturbance can be seen only below the tropopause. The vertical structure shown by Fig. 3 does not conflict with this theory. These facts indicate that the cyclone along the Himalayas is a TRW.

In order to discuss the formation mechanism of the TRW cyclone, we also conducted some numerical simulations using a simple f-plane shallow water equations system (SWEM). In the equations system, there are no waves except for topographic Rossby waves and gravity waves. The equations system used in SWEM is as follows,

$$\frac{\partial u}{\partial t} + u\frac{\partial u}{\partial x} + v\frac{\partial u}{\partial y} - f_0 v = -g^*\frac{\partial h}{\partial x} \qquad (3)$$

$$\frac{\partial v}{\partial t} + u\frac{\partial v}{\partial x} + v\frac{\partial v}{\partial y} + f_0 u = -g^*\frac{\partial h}{\partial y} \qquad (4)$$

$$\frac{\partial h}{\partial t} + \frac{\partial u \cdot (h - h_B)}{\partial x} + \frac{\partial v \cdot (h - h_B)}{\partial y} = 0, \quad (5)$$

where h is the level of the water surface, h_B is the elevation of the bottom, g^* is the reduced gravity which is assuming to be 1.0 m/s^2, and f_0 is the Coriolis parameter. The orography is assumed to be a cigar-shape whose width is 10,000 km along the meridional direction and 3,000 km in the latitudinal direction and maximum height is 3,000 m (shaded area in Figure 4). After the mountain waves achieved a stationary state, a trough is artificially created in the windward of the mountain. The trough is meridionally uniform and has been adjusted to be geostrophic balance.

Figure 4 shows the elevation of the water surface simulated by SWEM at every 30 hours after the start of the simulation. The initial state is shown in Figure 4A. When the trough passes through the orography, the trough is divided into two parts by the orography (Figure 4B), and two cyclonic circulation patterns appear in the northern and southern side of the orography (Figure 4C). The northern cyclone moves faster than the speed of the westerly, but the southern cyclone moves very slowly and seems to be almost stationary. These properties of the cyclones agree with observation and the realistic simulation shown above.

As well as the numerical model with full physics, SWEM can also almost completely simulate formation process in which a cyclone is separated from a synoptic trough by the Tibetan plateau and propagates slowly eastward along the southern slope of the Himalayas.

The model experiments also show that the cyclone along the southern slope can exist only when the phase speed of the TRW is slower than the wind speed of the westerly. This demonstrates the existence of the threshold westerly velocity. When the westerly is less that the threshold, any disturbances induced by the trough cannot propagate to the southern side of the orography. Since the threshold velocity is roughly esti-
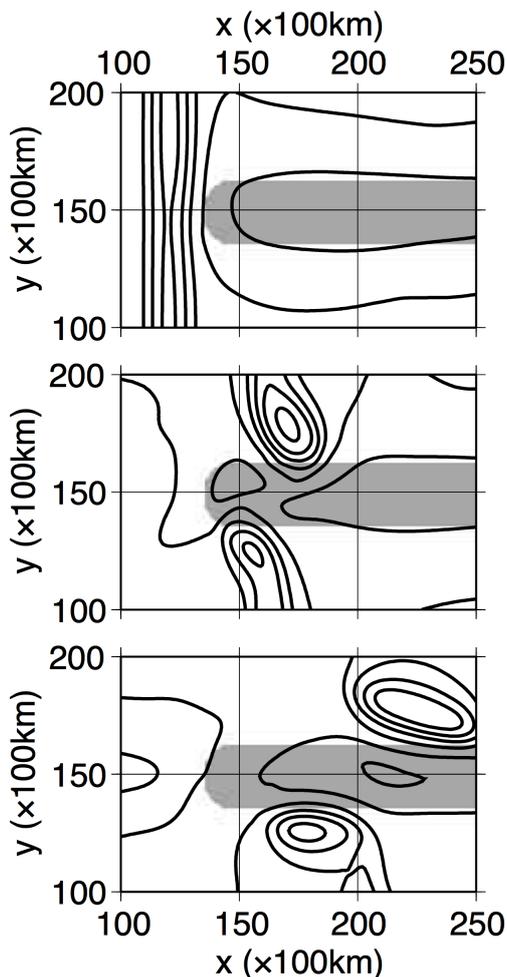
Figure 4: Fluid height of the SWEM in (A) 36 hours, (B) 72 hours, and (C) 108 hours. The contour lines indicate the fluid height, and the shaded area indicates the area in which the orographic height is greater than 2500 m.

mated to be about 20 m/s in the Himalayas, the TRW cyclone forms in the case of relatively strong westerly. The threshold velocity depends on the size of the TRW and the steepness of the slope.

4   Summary

A quasi-stationary cyclone was observed over the southern slope of the Himalayas. This cyclone can be explained as a TRW along the Himalayan slope since it can be simulated well by full-parameterized numerical models as well as by a simple SWEM. The phase speed and vertical and horizontal structure of the cyclone agree well with the linear theory of TRWs.

Similar cyclones have been observed at least three times (February 8 to 12 1996, February 23 to 25 1998, and December 5 to 10 1999) from 1995 to 1999. All cyclones were observed in winter and slowly propagated along the southern slope of the Tibetan plateau. Since these cyclones sometimes bring heavy snowfall along the Himalayan range and the southern part of the Tibetan plateau, further understanding of the dynamics of their genesis, growth, and decay is essential for the prediction and prevention of snow disasters in these regions.

References

[1] Hsu, H.-H. (1987), Propagation of Low-Level Circulation Features in the Vicinity of Mountain Ranges, *Mon. Wea. Rev.*, *115*, 1864–1892.

[2] Gill, A. E. (1977), Coastally Trapped Waves in the Atmosphere, *Quart. J. R. Met. Soc.*, *103*, 431–440.

[3] Gross, B. D.(1994), Frontal Interaction with Isolated Orography, *J. Atmos. Sci.*, *51*, 1480–1496.

[4] Kalnay, E. and co-authors (1996), The NCEP/NCAR 40-Year Reanalysis Project, *Bull. Amer. Meteor. Soc.*, *77*, 437–472.

[5] Lang, T. J. and A. P. Barros (2004), Winter Storms in the Central Himalayas, *J. Meteor. Soc. Japan*, *82*, 829–844.

[6] Nakamura, H. and T. Doutani (1985), A Numerical Study on the Coastal Kelvin Wave Features about the Cold Surges around the Tibetan Plateau, *J. Meteor. Soc. Japan*, *63*, 547–563.

[7] Pedlosky, J. (1987), *Geophysical Fluid Dynamics*, 2nd ed., 710 pp., Springer-Verlag, New York.

[8] Pielke, R. A. and co-authors (1992), A Comprehensive Meteorological Modeling System RAMS, *Meteorol. Atmos. Phys.*, *49*, 69–91.

[9] Reynolds, R. W. and T. M. Smith (1994), Improved Global Sea Surface Temperature Analysis Using Optimum Interpolation, *J. Climate*, *7*, 929–948.

[10] Rhines, P. B. (1969), Slow Oscillations in an Ocean of Varying Depth Part1. Abrupt Topography, *J. Fluid Mech.*, *37*, 161–189.

[11] Sakai, T. (1991), The Assault on Meilixueshan and Tragic Loss of Seventeen Climbers, *SANGAKU (The Journal of the Japanese Alpine Club)*, *86*, 104–111 (in Japanese with an English abstract).

[12] Sato, T. and F. Kimura (2003), A Two-dimensional Numerical Study on Diurnal Cycle of Mountain Lee Precipitation, *J. Atmos. Sci.*, *60*, 1992–2003.

[13] Sumi, A. (1985), A Study on Cold Surges Around the Tibetan Plateau by Using Numerical Models, *J. Meteor. Soc. Japan*, *63*, 377–396.

[14] Tory, K. J., P. L. Jackson, and C. J. C. Reason (2001), Sensitivity of Coastally Trapped Disturbance Dynamics to Barrier Height and Topographic Variability in a Numerical Model, *Mon. Wea. Rev.*, *129*, 2955–2969.

[15] Yoshikane, T., F. Kimura, and S. Emori (2001), Numerical Study on the Baiu Front Genesis by Heating Contrast between Land and Ocean, *J. Meteor. Soc. Japan*, *79*, 671-686.